Journal of Computational and Applied Mathematics 227 (2009) 17–26

Contents lists available at ScienceDirect

Journal of Computational and Applied Mathematics

journal homepage: www.elsevier.com/locate/cam

Application of the GALI method to localization dynamics in nonlinear systems☆

T. Bountis [a,*], T. Manos [a,b], H. Christodoulidi [a]

[a] Center for Research and Applications of Nonlinear Systems (CRANS), Department of Mathematics, University of Patras, GR–26500, Patras, Greece

[b] Laboratoire d'Astrophysique de Marseille (LAM), Observatoire Astronomique de Marseille-Provence (OAMP), 2 Place Le Verrier, F–13248, Marseille, France

ARTICLE INFO

Article history:
Received 23 February 2008

We dedicate this paper to Professor Apostolos Hadjidimos, whose inspiring research and teaching all these years has demonstrated that Numerical Analysis is a truly fundamental branch of Mathematics and not simply a useful tool for solving scientific problems.

Keywords:
Hamiltonian systems
Discrete breathers
Symplectic maps
Standard map
Chaotic motion
Quasiperiodic motion
GALI method
Dimension of tori

ABSTRACT

We investigate localization phenomena and stability properties of quasiperiodic oscillations in N degree of freedom Hamiltonian systems and N coupled symplectic maps. In particular, we study an example of a parametrically driven Hamiltonian lattice with only quartic coupling terms and a system of N coupled standard maps. We explore their dynamics using the Generalized Alignment Index (GALI), which constitutes a recently developed numerical method for detecting chaotic orbits in many dimensions, estimating the dimensionality of quasiperiodic tori and predicting slow diffusion in a way that is faster and more reliable than many other approaches known to date.

1. Introduction

In the present paper, we apply the Generalized Alignment Index (GALI) method introduced in [12] to two types of dynamics, which are related to localization phenomena in multi-dimensional Hamiltonian systems and symplectic maps. The first type refers to quasiperiodic oscillations in the vicinity of what is known as *discrete breathers*, or exact periodic solutions of multi-dimensional systems, which are exponentially localized in real space. The second class of phenomena concerns localization in Fourier space and is evidenced by the persistence of quasiperiodic recurrences in the neighborhood of normal mode oscillations of nonlinear lattices, observed for example in the famous numerical experiments performed by Fermi Pasta and Ulam (FPU) in the early 1950's [3,5,6,1].

In Section 2, we present a brief introduction to the GALI method and in Section 3 we use it to study quasiperiodic motion on tori of low dimensionality near a stable discrete breather of a Hamiltonian lattice, with nonlinear on site potential and only quartic nearest neighbor interactions. Then in Section 4, we turn to a system of N coupled standard maps and give

☆ Invited paper.

* Corresponding author.
E-mail address: bountis@math.upatras.gr (T. Bountis).
URL: http://www.math.upatras.gr/bountis/ (T. Bountis).

0377-0427/$ – see front matter © 2009 Published by Elsevier B.V.
doi:10.1016/j.cam.2008.07.034

evidence for the existence of both of the above types of localization: First starting with initial conditions localized in real space, we find low dimensional quasiperiodic motion, which persists for very long times. We also study in this discrete model recurrences of its (linear) normal mode oscillations and find that, just like the FPU model, the tori associated with them are low-dimensional, despite the fact that, unlike the FPU example, each oscillator contains on site nonlinear terms, which depend on its individual variables. Finally we discuss our conclusions in Section 5.

2. Definition of the GALI method

Let us consider the $2N$-dimensional phase space of a conservative dynamical system, which may be represented by a Hamiltonian flow of N degrees of freedom or a $2N$-dimensional system of coupled symplectic maps. In order to study whether an orbit is chaotic or not, we examine the asymptotic behavior of k initially linearly independent deviations from this orbit, denoted by the vectors $\vec{v}_1, \vec{v}_2, \ldots, \vec{v}_k$ with $2 \leq k \leq 2N$. Thus, we follow the orbit, using Hamilton's equations (or the map equations) of motion and solve in parallel the variational equations about this orbit to study the behavior of solutions located in its neighborhood.

The Generalized Alignment Index of order k is a generalization of the Smaller Alignment Index (SALI) introduced in [11] and is defined as the norm of the wedge (or exterior) product of k associated unit deviation vectors [12]:

$$\mathrm{GALI}_k(t) = \|\hat{v}_1(t) \wedge \hat{v}_2(t) \wedge \cdots \wedge \hat{v}_k(t)\| \tag{1}$$

representing *the volume of the parallelepiped*, whose edges are these k vectors. We note that the hat ($\hat{}$) over a vector denotes that it is of unit magnitude and that t represents the continuous or discrete time.

In the case of a chaotic orbit, all deviation vectors tend to become *linearly dependent*, aligning in the direction of the eigenvector corresponding to the maximal Lyapunov exponent and GALI_k tends exponentially to zero following the law [12]:

$$\mathrm{GALI}_k(t) \propto \mathrm{e}^{-[(\sigma_1-\sigma_2)+(\sigma_1-\sigma_3)+\cdots+(\sigma_1-\sigma_k)]t}, \tag{2}$$

where $\sigma_1 > \cdots > \sigma_k$ are approximations of the first k largest Lyapunov exponents of the dynamics. In the case of regular motion, on the other hand, all deviation vectors tend to fall on the N-dimensional tangent space of the torus, where the motion is quasiperiodic. Thus, if we start with $k \leq N$ general deviation vectors, these will remain *linearly independent* on the N-dimensional tangent space of the torus, since there is no particular reason for them to become aligned. As a consequence, GALI_k in this case remains practically constant for $k \leq N$. On the other hand, for $k > N$, GALI_k tends to zero, since some deviation vectors will eventually become *linearly dependent*, following power laws that depend on the dimensionality of the torus. According to our asymptotic analysis of determinants entering in an expansion of (1) in a basis of eigenvectors following the motion, one obtains the following formula for the GALI_k, associated with quasiperiodic orbits lying on m-dimensional (mD) tori [4]:

$$\mathrm{GALI}_k(n) \propto \begin{cases} \text{constant}, & \text{if } 2 \leq k \leq m \\ \dfrac{1}{t^{k-m}}, & \text{if } m < k \leq 2N - m \\ \dfrac{1}{t^{2(k-N)}}, & \text{if } 2N - m < k \leq 2N. \end{cases} \tag{3}$$

The computation of such determinants, however, is hardly the most efficient way to compute the GALI_k, especially in cases where the dimension of the system N becomes large. For this reason, we have recently introduced and employed a method based on Singular Value Decomposition to show that the GALI_k can be very efficiently computed as the product of the singular values of a $2N \times k$ matrix [2].

3. Applications to the dynamics near discrete breathers

In this section we examine the dynamics in the vicinity of discrete breathers in a one-dimensional Hamiltonian lattice with quartic on site potential and linear dispersion terms in its nearest neighbor particle interactions. For this purpose, we start with initial conditions near the exact breather and check whether the motion remains quasiperiodic or becomes chaotic. We accomplish this by computing the GALI indices along the reference orbit. If the breather is stable, the GALI method can be used to determine the dimensionality of the tori surrounding the breather in the $2N$-dimensional phase space. This dimension is generically N and equals the number of frequencies that are being excited in the neighborhood of the exact breather. As for chaotic motion diffusing slowly away from these breathers, it is rapidly and efficiently predicted by the exponential convergence of all GALI indices to zero. Let us take, for example, a Hamiltonian lattice of anharmonic oscillators, which involves only quartic coupling terms and hence presents strong localization phenomena due to the absence of phonons [7]. More specifically, we study here a system with on site potential: $V(x) = \frac{1}{2}[1-\varepsilon\cos(\omega_d t)]x^2 - \frac{1}{4}x^4$, described by the Hamiltonian [9]:

$$H(t) = \sum_n \left\{ \frac{1}{2}\dot{x}_n^2 + \frac{1}{2}[1 - \varepsilon\cos(\omega_d t)]x_n^2 - \frac{1}{4}x_n^4 + \frac{K}{4}(x_{n+1} - x_n)^4 \right\}, \tag{4}$$

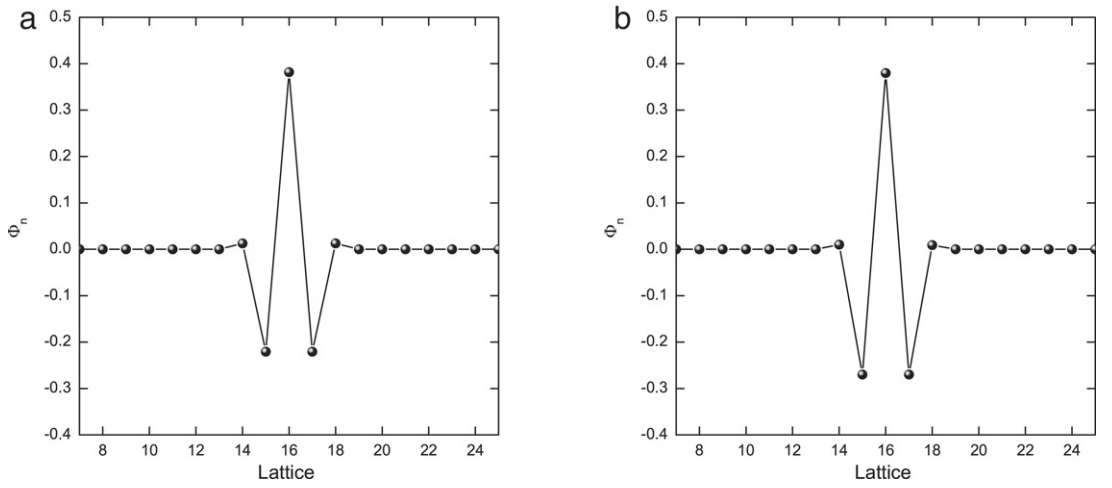

Fig. 1. (a) Initial conditions for the 31 particle lattice, obtained from homoclinic intersections of the spatial map Φ_n with all velocities set to zero. Here $D = 1$, representing a quasiperiodic breather (Case I in the text). (b) We now perturb the initial conditions, so that the amplitudes of the central particle and its 2 neighbors are slightly different from those in (a) (Case II in the text).

where ε, ω_d are the amplitude and frequency of the driver respectively. The equations of motion of each oscillator clearly are:

$$\ddot{x}_n = K(x_{n+1} - x_n)^3 + K(x_{n-1} - x_n)^3 - [1 - \varepsilon\cos(\omega_d t)]x_n + x_n^3. \tag{5}$$

It can be shown that the solutions of Eq. (5) can be written as a product of a time-dependent function $G(t)$ and a map Φ_n, depending only on the oscillation site n:

$$x_n(t) = \Phi_n G(t), \tag{6}$$

$n = 1, 2, \ldots, N$. Substituting (6) in (5), one finds that the equations of motion can be exactly separated into a spatial and a time-dependent part each of which is equal to an arbitrary constant C. Thus, we arrive at a periodically driven Duffing equation:

$$\ddot{G} + [1 - \varepsilon\cos(\omega_d t)]G = -CG^3, \tag{7}$$

satisfied by $G(t)$ and a discrete map:

$$C\Phi_n + K(\Phi_{n+1} - \Phi_n)^3 + K(\Phi_{n-1} - \Phi_n)^3 + \Phi_n^3 = 0, \tag{8}$$

which yields the spatial evolution of the system (4). Following [9], we consider a lattice of 31 particles, with $C = 1, K = 1, \varepsilon = 0.7$ and $\omega_d = 2.6355$. The initial conditions of the driven Duffing equation are chosen on an exact exact periodic orbit with $G(0) = D, \dot{G}(0) = 0$ and frequency $\omega_b = \omega_d/2$, if $D = D_b = \pm 1.2043$. Furthermore, if the initial conditions lie on the *homoclinic intersections* of the invariant manifolds of the saddle point at the origin of the map, the solution becomes an exact breather with $x_n(0) = \Phi_n D_b$, which is *linearly stable* [9].

Our first goal, therefore, is to examine the motion near this breather by perturbing the initial conditions in its neighborhood and applying the GALI indices to characterize the resulting orbits. In this study, we have made two kinds of perturbations: In the first case we change only the factor D, while in the second both the factor D and the spatial initial conditions of the map are varied.

Case I:

Let us start by perturbing the initial conditions $G(0) = D$ ($\dot{G}(0) = 0$) away from $D = D_b = 1.2043,$, while the initial conditions of Φ_n are fixed (Fig. 1(a)). In our example, we use a 31 particle Hamiltonian, with $C = 1, \varepsilon = 0.7$ and $\omega_d = 2.6355$.

Decreasing the value of $D < D_b$, we observe that the oscillations for $D = 1.1$ are quasiperiodic and remain so for long integration times, while the particles oscillate with frequencies close to that of the exact breather, as shown in Fig. 2. This is in agreement with the fact that even $GALI_2$ (representing the area of the parallelogram formed by the two unit deviation vectors) tends to zero following the power law t^{-1}. When D becomes 0.9, the $GALI_k$ indices begin to fluctuate, indicating that the orbit is near the edge of the corresponding regular region in phase space (Fig. 2(c)). Moreover, near $t = 10^6$, $GALI_2$ begins to tend to a constant value, suggesting that the motion has become quasiperiodic with 3 frequencies. Finally, as D reaches the value 0.8, quasiperiodic recurrences break down and the motion becomes chaotic.

Case II:

We now slightly perturb the initial conditions of the discrete map Φ_n (as indicated in Fig. 1(b)) and observe that the motion now occurs on a 3D torus, indicating the appearance of 3 frequencies in the system. This quasiperiodic breather

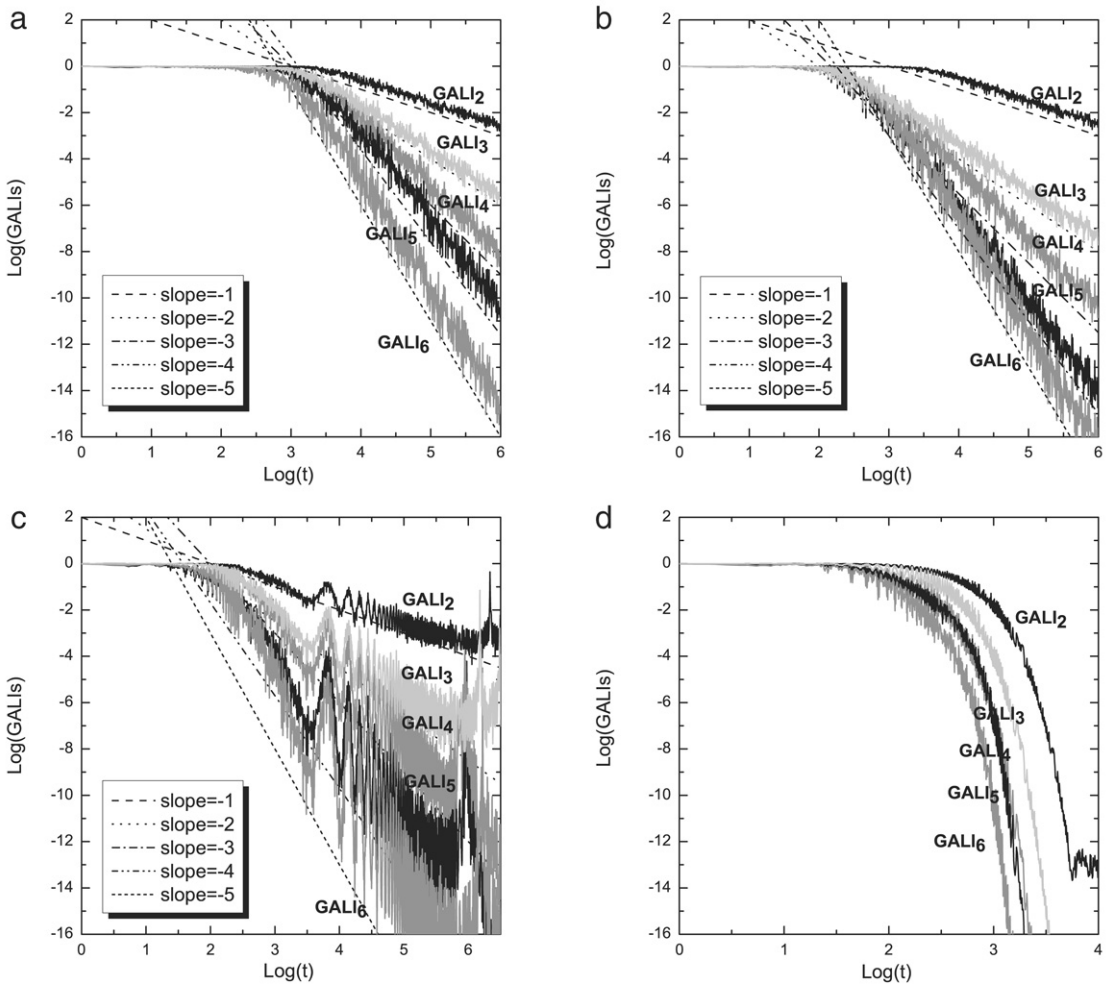

Fig. 2. Time evolution of $GALI_k$ indices for: (a) $D = 1.1$ and initial energy $H(0) = 0.133$, see (4), (b) $D = 1$ and $H(0) = 0.097$, (c) $D = 0.9$ and $H(0) = 0.07$ and (d) for $D = 0.8$ and $H(0) = 0.048$. Notice that in (a) and (b) the breather remains quasiperiodic for very long times, lying on a one-dimensional torus, which implies that only one main frequency is excited. In (c) the motion lies on a 3D torus as $GALI_2$ and $GALI_3$ tend to a non-zero value, while in (d) the motion is evidently chaotic and delocalizes, drifting away from the breather. The slopes of $GALI_k$ evolution coincide with the laws presented in formulas (2) and (3).

behavior lies on a 3D torus, in phase space, as D varies from 0.75 to 1 (Fig. 3). In fact, for $1 < D < 1.2$, the chaotic character of the orbit is revealed by the exponential decay of all $GALI_k$ indices.

For $D = 1.2$, in fact, recurrences break down and delocalization sets in, as particles away from the center of the lattice gain energy and begin to oscillate (see Fig. 4(d)). The exponential convergence of GALI indices to zero indicates the chaotic behavior of the motion. Fig. 4(a) shows that there are only three positive Lyapunov exponents, indicating three instability directions about the orbit in phase space. The exponents σ_1 and σ_2 are almost identical, having a difference of the order 10^{-5} (Fig. 4(b)). As a consequence, $GALI_2 \propto e^{-(\sigma_1-\sigma_2)t}$ begins to converge exponentially when t becomes greater than 10^{-5}, while the other GALIs have reached the value 10^{-16} exponentially, long before 10^4 (see Fig. 4(c)).

4. Application to the dynamics of *N* coupled standard maps

The standard map, also referred to as the Chirikov–Taylor map [8], is an area preserving map, which appears in many physical problems. It is defined by the equations:

$$\begin{aligned} x_{n+1} &= x_n + y_{n+1}, \\ y_{n+1} &= y_n + K \sin(x_n), \end{aligned} \tag{9}$$

where both variables are taken modulo one in the unit square. This map describes the motion of a simple mechanical system called a kicked rotator. It may be thought of as representing a pendulum rotating on a horizontal frictionless plane around a fixed axis and being periodically kicked by a nonlinear force at the other end, at unit time intervals. The variables x_n and y_n

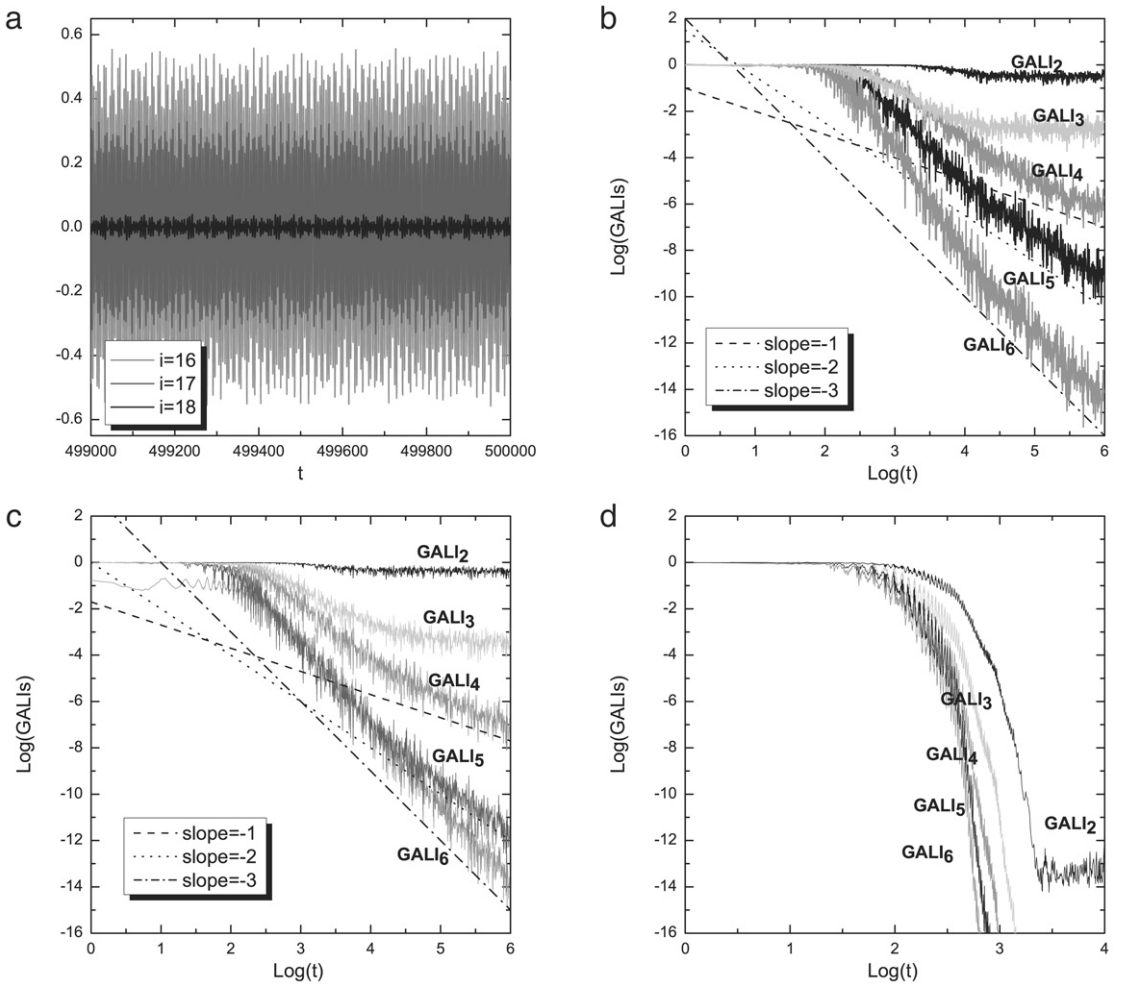

Fig. 3. (a) Oscillations of particles 16, 17, 18 of the lattice show the localization and quasiperiodic properties of the motion near the discrete breather. This is verified by the time evolution of $GALI_k$ indices in (b) for $D = 0.9$ and $H(0) = 0.09$ and in (c) for $D = 0.8$ and $H(0) = 0.062$, showing the orbits lie on a 3-dimensional torus. However, in (d) we take $D = 0.7$ and $H_0 = 0.042$, perturbing the initial conditions as shown in Fig. 1(b). Here, the slopes of the $GALI_k$ indices clearly demonstrate that the motion chaotically diffuses away.

determine, respectively, the angular position of the pendulum and its angular momentum after the nth kick. The constant K measures the intensity of the nonlinear "kicks".

The standard map describes many other systems occurring in the fields of mechanics, accelerator physics, plasma physics, and solid state physics. However, it is also interesting from a fundamental point of view, since it is a very simple model of a Hamiltonian system of 2 degrees of freedom that displays order and chaos.

For $K = 0$, the map is linear and only periodic and quasiperiodic orbits are allowed (depending on the value of y_0), which fill horizontal straight lines in the x_n, y_n phase plane of the map. However, when $K \neq 0$, the periodic lines break into pairs of isolated points half of which are stable and half unstable alternatingly. The stable periodic points possess families of quasiperiodic orbits forming closed curves around them, while the unstable ones are saddles with thin chaotic layers close to their invariant manifolds. Moreover, as $K > 0$ grows, the size of the chaotic layers increase and occupy larger and larger regions of the available phase plane [8,10], see Fig. 5.

Let us consider a system of N coupled standard maps described by the following equations:

$$\begin{aligned} x^j_{n+1} &= x^j_n + y^j_{n+1}, \\ y^j_{n+1} &= y^j_n + \frac{K_j}{2\pi}\sin(2\pi x^j_n) - \frac{\beta}{2\pi}\{\sin[2\pi(x^{j+1}_n - x^j_n)] + \sin[2\pi(x^{j-1}_n - x^j_n)]\} \end{aligned} \tag{10}$$

with $j = 1, \ldots, N$, fixed boundary conditions $x_0 = x_{N+1} = 0$ and β the coupling parameter between neighboring maps. In what follows, we shall examine the localization properties of this system comparing the dynamics with what is observed when one studies a one-dimensional Hamiltonian system like the FPU lattice.

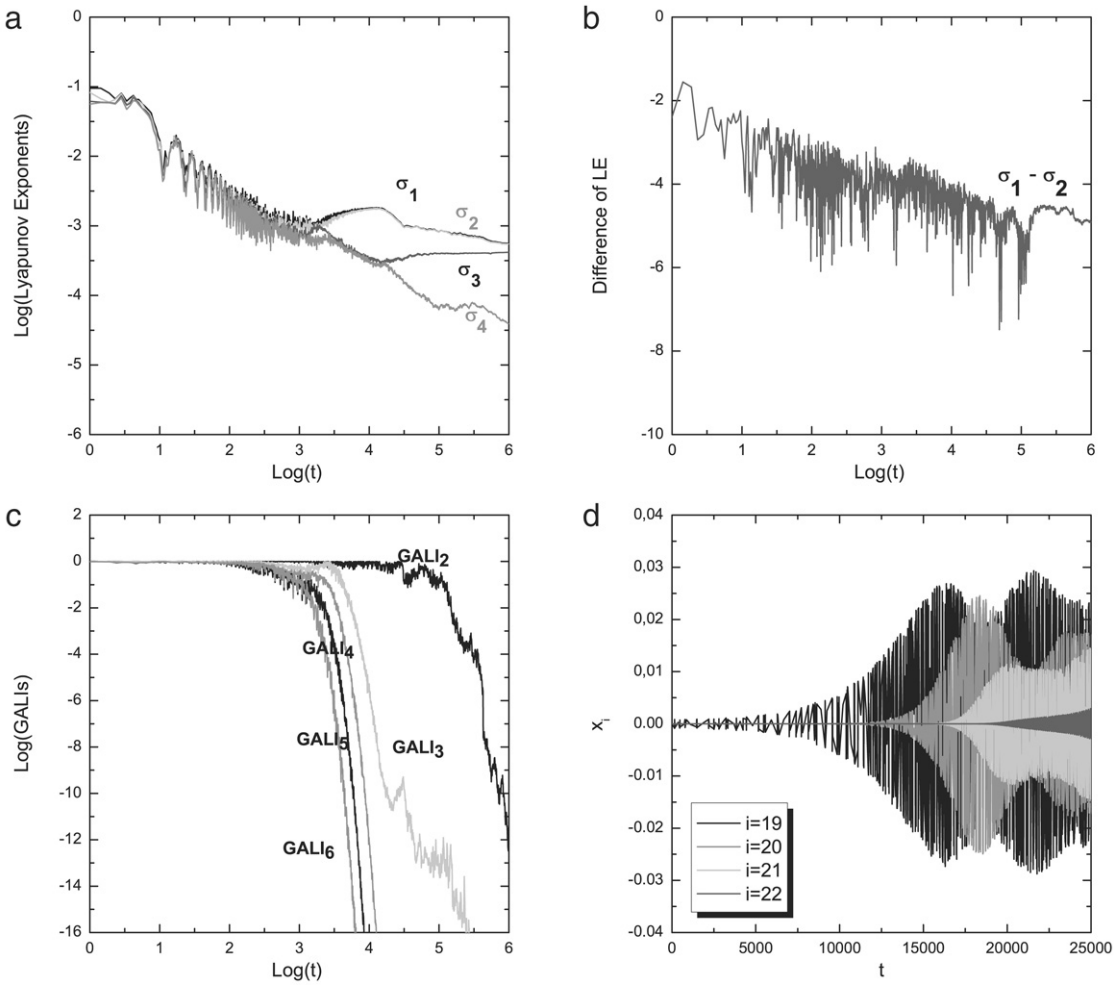

Fig. 4. When we choose initial conditions as shown in Fig. 1(b) (Case II), we find that with $D = 1.2$ recurrences break down, while (a) the four largest Lyapunov exponents appear to be decreasing to zero. Note in (b) that the difference between the two largest Lyapunov exponents, $\sigma_1 - \sigma_2$, is nonzero and tends to a constant, explaining why in (c) we observe exponential behavior of $GALI_k$. (d) This agrees with the fact that the particles away from the center of the lattice start to oscillate, indicating delocalization and the breakdown of recurrency.

4.1. Initial conditions localized in real space

Let us begin with the question of the existence of stable discrete breathers in this model, when the coupling parameter β is small. Note that our equations have an exact stable fixed point, when all particles are located at $(x, y) = (0.5, 0.0)$ (see Fig. 5). Taking $N = 20$ coupled standard maps, we may, therefore, look for localized oscillations taking as initial condition (R1): $(x_j, y_j) = (0.5, 0.0)$, $\forall j \neq 11$, perturbing only one particle at $(x_{11}, y_{11}) = (0.65, 0.0)$ and fixing the parameters $\beta = 0.001$, setting $K_j = 2$, with $j = 1, \ldots, 20$. If a stable discrete breather exists, the orbits are expected to oscillate about these initial conditions quasiperiodically for very long times.

Indeed, when we evaluate the $GALI_k$ indices for $n = 10^6$ iterations in Fig. 6(a) and display their evolution for $k = 2, \ldots, 7$ on a logarithmic scale, we find that $GALI_2$ fluctuates around a non-zero value while all the other GALIs decay to zero following power laws. This implies that the motion is that of a quasiperiodic orbit that lies on a 2-dimensional (2D) torus. In fact, for initial conditions (R2): $(x_j, y_j) = (0.5, 0.0)$, $\forall j \neq 11, 12$, perturbing two particles $(x_{11}, y_{11}) = (0.65, 0.0)$, $(x_{12}, y_{12}) = (0.55, 0.0)$ for the same parameters as in the R1 experiment, we detected regular motion that lies on a 3D torus! This is demonstrated by the evolution of the GALIs in Fig. 6, where not only $GALI_2$ but also $GALI_3$ fluctuates around a non-zero value.

Such localized regular dynamics becomes evident in Fig. 6(c), where we exhibit the oscillations of the x_n-coordinate of the 11th, 12th and 13th maps of the system for the last 10^5 iterations of the R2 experiment. As seen in the figure, the motion is indeed quasiperiodic and confined to the middle 3 maps, as all other degrees of freedom do not gain any significant amount of energy. Similarly, we have observed that exciting 3 central particles ($j = 10, 11, 12$) gives a quasiperiodic motion on 4D tori. This is reminiscent of the motion near discrete breathers of Hamiltonian systems and suggests that the excitation of each particle adds one extra frequency to the motion.

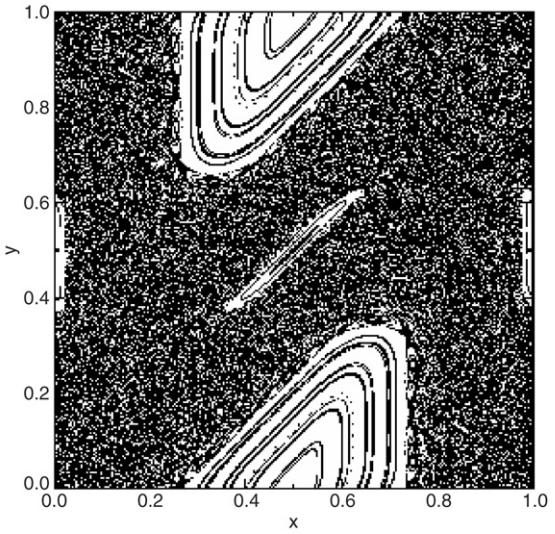

Fig. 5. Poincaré surface of section of a single standard map for $K = 2$. Note the presence of a stable fixed point at $(x, y) = (0.5, 0.0)$ (and its modulo equivalent at $(x, y) = (0.5, 1.0)$), surrounded by a large "island" of quasiperiodic orbits. The smaller islands embedded in the large chaotic "sea" correspond to a stable periodic orbit of period 2.

4.2. Initial conditions localized in Fourier space

Finally, let us investigate the phenomenon of FPU recurrences in our system of coupled standard maps. To do this, we first need to derive the linear normal modes of the model, in order to choose initial conditions that will excite only a small number of them. Thus, keeping only the first term in the Taylor expansion of the *sine*-function in (10), we obtain the following system of equations:

$$x' = \mathcal{A}x, \tag{11}$$

where $x' = (x^1_{n+1}, y^1_{n+1}, \ldots, x^N_{n+1}, y^N_{n+1})^{\mathrm{T}}$, $x = (x^1_n, y^1_n, \ldots, x^N_n, y^N_n)^{\mathrm{T}}$ and

$$\mathcal{A} = \begin{bmatrix}
K_1+\gamma & 1 & -\beta & 0 & \ldots & 0 & 0 & 0 & 0 & 0 \\
K_1+2\beta & 1 & -\beta & 0 & \ldots & 0 & 0 & 0 & 0 & 0 \\
-\beta & K_2+\gamma & 1 & -\beta & \ldots & 0 & 0 & 0 & 0 & 0 \\
-\beta & K_2+2\beta & 1 & -\beta & \ldots & 0 & 0 & 0 & 0 & 0 \\
\vdots & \vdots & \vdots & \vdots & & \vdots & \vdots & \vdots & \vdots & \\
0 & 0 & 0 & 0 & \ldots & -\beta & K_{N-1}+\gamma & 1 & -\beta & 0 \\
0 & 0 & 0 & 0 & \ldots & -\beta & K_{N-1}+2\beta & 1 & -\beta & 0 \\
0 & 0 & 0 & 0 & \ldots & 0 & 0 & -\beta & K_N+\gamma & 1 \\
0 & 0 & 0 & 0 & \ldots & 0 & 0 & -\beta & K_N+2\beta & 1
\end{bmatrix}, \tag{12}$$

with $\gamma = 1 + 2\beta$.

Using now well-known methods of linear algebra, we diagonalize the matrix $\mathcal{A}$ writing $\mathcal{D} = \mathcal{P}^{-1}\mathcal{A}\mathcal{P}$, where $\mathcal{P}$ is an invertible matrix whose columns are the eigenvectors of the matrix $\mathcal{A}$ and $\mathcal{D}$ is diagonal, $\mathcal{D} = \mathrm{diag}[\lambda_1, \ldots, \lambda_{2N}]$, provided the eigenvalues λ_i are real and discrete.

Our case, of course, involves oscillations about a stable equilibrium point and hence the above system has $2N$ discrete complex eigenvalues $\lambda_j = a_j + \mathrm{i}b_j$, $\bar{\lambda}_j = a_j - \mathrm{i}b_j$ and eigenvectors $w_j = u_j + \mathrm{i}v_j$, $\bar{w}_j = u_j - \mathrm{i}v_j$, with $j = 1, 2, \ldots, N$. Thus, $u_1, v_1, \ldots, u_N, v_N$ form a basis of the space $\mathcal{R}^{2N}$ and the invertible matrix $\mathcal{P} = [v_1, u_1, , \ldots, v_N, u_N]$ leads us to the Jacobi normal form:

$$\mathcal{B} = \mathcal{P}^{-1}\mathcal{A}\mathcal{P} = \mathrm{diag}\begin{bmatrix} a_j & -b_j \\ b_j & a_j \end{bmatrix},$$

of a $2N \times 2N$ matric $\mathcal{B}$ with 2×2 blocks along its diagonal. In this way, using the transformation $z = \mathcal{P}^{-1}x$, we can reduce the initial problem to a system of uncoupled equations, whose evolution is described by the equations:

$$z' = \mathcal{P}^{-1}\mathcal{A}\mathcal{P}z, \tag{13}$$

where $z' = (l^1_{n+1}, k^1_{n+1}, \ldots, l^N_{n+1}, k^N_{n+1})^{\mathrm{T}}$, $z = (l^1_n, k^1_n, \ldots, l^N_n, k^N_n)^{\mathrm{T}}$ and z represents the linear normal modes of the map. Thus, in order to excite a continuation of one or more of these modes, we extract the appropriate x-initial condition by the

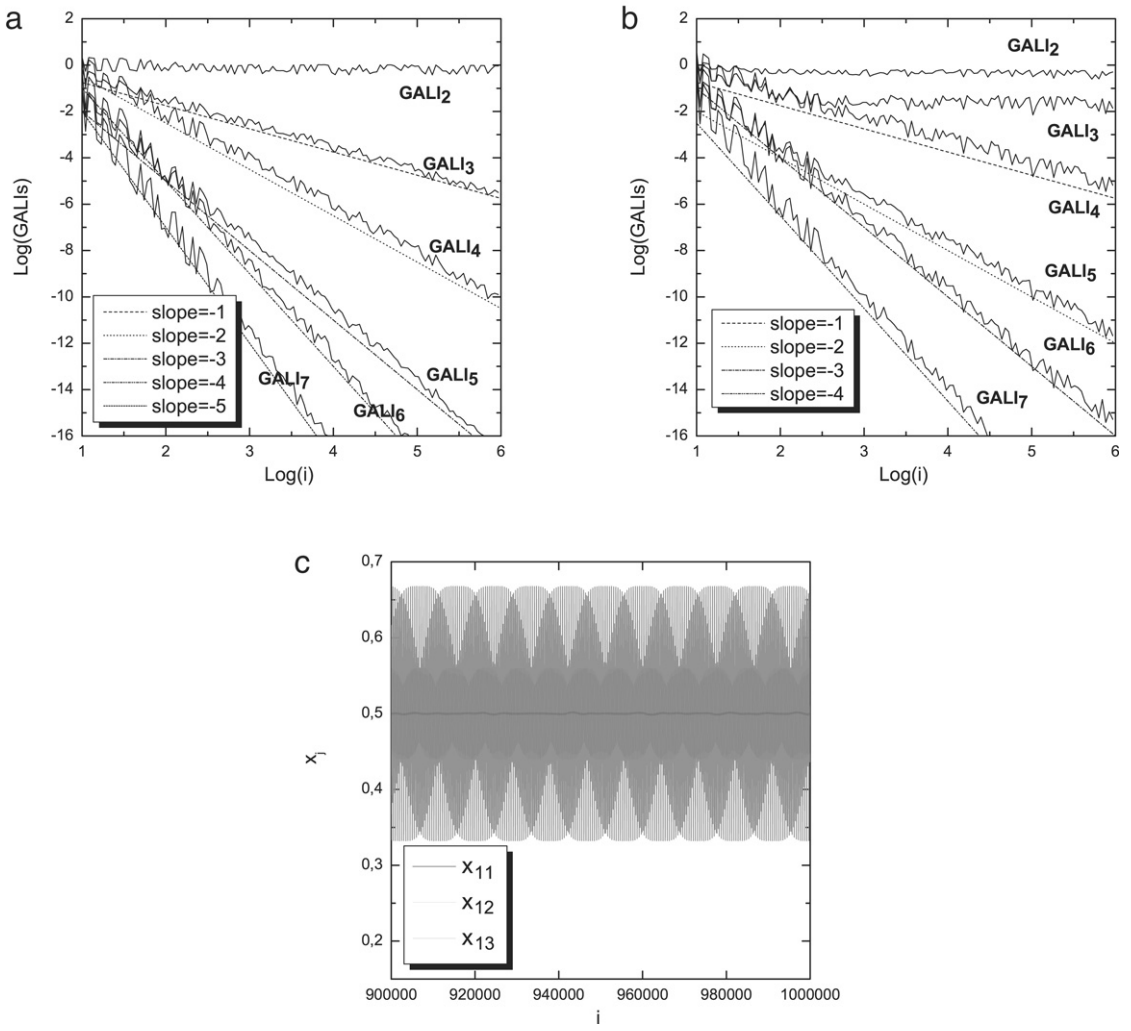

Fig. 6. (a) GALI_k, $k = 2, \ldots, 7$, for $N = 20$ – coupled standard maps with $K_j = 2$, $\beta = 0.001$ and initial conditions R1 (see text). GALI_2 fluctuates around a non-zero value implying a regular motion that lies on a 2D torus, while the slopes of the algebraically decaying indices are in agreement with (3).(b) GALI_k for the initial conditions R2 (see text) imply that the motion lies on a 3D torus, since $\mathrm{GALI}_{2,3}$ tend to a non-zero number. This quasiperiodic localized dynamics of R2 is clearly seen in (c), where we plot the x_n oscillations of the 11th (light gray color), 12th (gray color) and 13th (black color) map. From the last 10^5 iterations shown in this figure, it is evident that the main part of the energy is confined only in the "middle" 3 maps and is not shared by any of the other degrees of freedom of the system.

transformation $x = \mathcal{P}z$. The evolution in the uncoupled coordinates is given by the transformation:

$$\begin{aligned} l^j_{n+1} &= a_i l^j_n - b_i k^j_n \\ k^j_{n+1} &= b_i l^j_n + a_i k^j_n \end{aligned} \tag{14}$$

where each pair of (l^j, k^j) corresponds to a normal mode of the system. Since the map is area-preserving $a_j^2 + b_j^2 = 1$, we may define the quantity $E^j_n = (l^j_n)^2 + (k^j_n)^2$ as the energy of each mode, which is preserved under the evolution of the linear map, i.e. $E^j_{n+1} = E^j_n$.

Thus, to study recurrences, we start with the example of $N = 5$ coupled standard maps, choose a 'small' coupling parameter $\beta = 0.00001$ and excite 5 different modes. As a result, we are able to detect a quasiperiodic orbit that lies on a 5D torus, indicated by all the GALI_k, $k = 1, \ldots, 5$, approaching a constant, as shown in Fig. 7(a). This is verified in Fig. 7(b), where we plot the corresponding energy modes of the coupled system and find that they are nearly invariant, as they would have been in the uncoupled case.

Next, we increase the number of coupled maps from 5 to 20, keeping $\beta = 0.00001$ and choosing different K_j (in triplets of $-1.35, -1.45, -1.55$), with $j = 1, \ldots, 20$. Exciting now only *one normal mode* (the 1st), much like the original FPU case, we calculate the GALIs again and find that the orbit is again quasiperiodic, lying on a 6-dimensional torus, as evidenced by the fact that GALI_k for $k = 2, \ldots, 6$ fluctuate around non-zero values, see Fig. 8(a). This is, of course, a low-dimensional

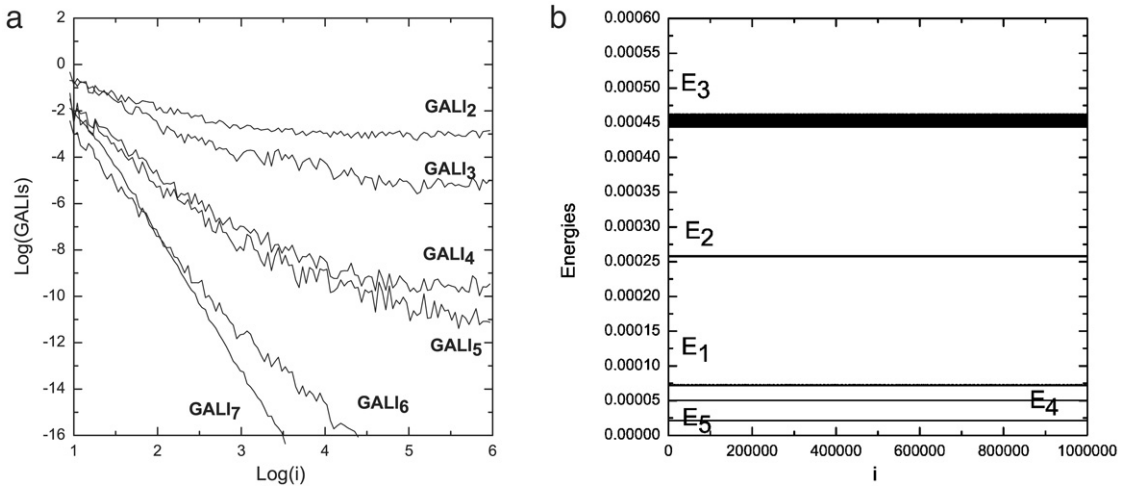

Fig. 7. (a) GALIs for 5 coupled standard maps with $K_1 = -2.30$, $K_2 = -2.35$, $K_3 = -2.40$, $K_4 = -2.45$, $K_5 = -2.50$, $B = 0.00001$ and initial conditions that excite 5 different normal modes. Note that the GALI_k for $k = 2, 3, 4, 5$ fluctuate around a non-zero value implying a regular motion that lies on a 5D torus. (b) The energies for the corresponding normal modes.

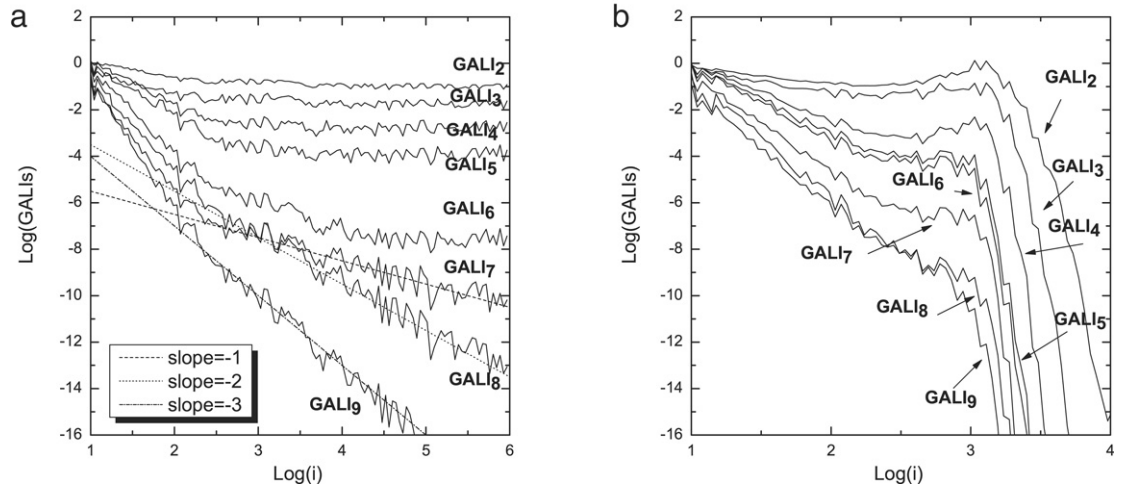

Fig. 8. (a) Exciting only one mode in a case of 20 coupled standard maps, with $\beta = 0.00001$ and K_j in triplets of -1.35, -1.45, -1.55, the GALI_k, for $k = 2, \ldots, 6$ asymptotically become constant, implying that the motion lies on a 6D torus. (b) An orbit with the same initial condition and K_j as in (a) but with a larger coupling parameter, ($\beta = 0.01$), becomes chaotic, as all the GALIs are seen to decay exponentially to zero.

torus, since generically one expects regular orbits of this system to lie on $N = 20$-dimensional tori! From the calculation of the normal mode energies in this experiment, we observe that the initial energy is now shared by 6 modes and executes recurrences, for as long as we have integrated the equations of motion. The energies of these 6 modes are not shown here since their values are too close to each other to be distinguished in a graphical representation.

Finally, as our last experiment, we increase the coupling parameter to $\beta = 0.01$, for the same choice of initial conditions and K_j values as in Fig. 8(a). The result is that the influence of the coupling is now quite strong and leads to the breakdown of recurrences and the onset of chaotic behavior. This is clearly depicted in Fig. 8(b), where the GALI_ks of this case exhibit exponential decay, implying the chaotic nature of this orbit.

5. Conclusions

Localized oscillations in one-dimensional nonlinear Hamiltonian lattices constitute, for the last 15 years, one of the most active areas of research in Mathematical Physics. Of primary interest has been the discovery of certain exact periodic solutions in such lattices, called discrete breathers, which are exponentially localized *in real space*. It is known that when these solutions are stable, there are regions around them in phase space, where orbits oscillate quasiperiodically for very long times, even though the presence of linear dispersion is expected to lead them to delocalization away from the discrete breather. How long do they stay, however, in that vicinity and what is the dimensionality of the tori on which they lie?

Furthermore, how large are these regular regions and at what initial conditions (or parameter values) does chaotic behavior begin to arise?

Similar questions can also be posed about another form of localization *in Fourier space*, which has been very recently proposed as an explanation of the famous recurrence phenomena known to characterize the dynamics near linear normal modes of nonlinear lattices, since the early 1950s. Clearly, the interest in such localization lies in the (in)ability of Hamiltonian lattices to exhibit energy propagation and equipartition as expected from the theory of statistical mechanics.

To answer such questions, we have applied in this paper a new method that our group has recently developed, which is able to distinguish order from chaos, identify the dimensionality of tori and predict slow diffusion in thin chaotic layers, faster and more reliably than other methods (see also our recent publication [13]). This is accomplished by computing what we call the *GALI indices* of the orbits under study, for which we have obtained analytical formulas that are in excellent agreement with numerical calculations.

We have thus considered two examples of high dimensional systems: One Hamiltonian lattice described by 31 Newton's second order differential equations and one system of 20 coupled area-preserving pairs of difference equations mapping the plane onto itself. In each of these models, we have been able to demonstrate the usefulness of the GALI indices in analyzing the properties of regular motion localized in real and Fourier space. Furthermore, we have shown that our indices can accurately determine cases where the motion becomes delocalized and starts to diffuse chaotically in phase space, long before this is observed in the actual oscillations.

We wish to emphasize the superiority of our approach to the traditional calculation of *Lyapunov exponents*, still used by many researchers to distinguish regular from chaotic motion. As we have shown, Lyapunov exponents can be misleading, as they often tend to decrease in time giving the impression that the motion is quasiperiodic, while it is in fact weakly chaotic. The GALI indices, on the other hand, are computationally more efficient, as they concentrate on the *tangent space* of the dynamics and explore the *linear (in)dependence* of k unit deviation vectors about an orbit representing the volume of their associated parallelepiped. If, for $k = 1, 2 \ldots, d$, that volume remains constant and decays for $k > d$ by well-defined power laws, the motion is quasiperiodic on a d-dimensional torus, while if the volume decreases exponentially for all k the motion is chaotic. We, therefore, hope that the virtues of the GALI method emphasized in this paper, will encourage researchers studying the dynamics of multi-dimensional conservative systems to use them to investigate many other physically interesting applications.

Acknowledgements

The authors wish to thank Dr. Haris Skokos and Dr.Christos Antonopoulos for many useful discussions on the topics of this paper. T. Manos was partially supported by the "Karatheodory" graduate student fellowship No B395 of the University of Patras, the program "Pythagoras II" and the Marie Curie fellowship No HPMT-CT-2001-00338. H. Christodoulidi was supported by the State Scholarships Foundation of Greece.

References

[1] Ch. Antonopoulos, T. Bountis, Stability of simple periodic orbits and chaos in a Fermi–Pasta–Ulam lattice, Phys. Rev. E 73 (2006) 056206.
[2] Ch. Antonopoulos, T. Bountis, Detecting order and chaos by the linear dependence index, ROMAI J. 2 (2) (2006) 1.
[3] G.P. Berman, F.M. Izrailev, Chaos 15 (2005) 015104.
[4] H. Christodoulidi, T. Bountis, Low-dimensional quasiperiodic motion in hamiltonian systems, ROMAI J. 2 (2) (2006) 37.
[5] S. Flach, A. Gorbach, Discrete breathers in Fermi–Pasta–Ulam lattices, Chaos 15 (2005) 1.
[6] S. Flach, M.V. Ivanchenko, O.I. Kanakov, q-Breathers in Fermi–Pasta–Ulam chains: Existence, localization and stability, Phys. Rev. E 73 (3) (2006) 036618.
[7] A.V. Gorbach, S. Flach, Compactlike discrete breathers in systems with nonlinear and nonlocal dispersive terms, Phys. Rev. E 72 (2005) 056607.
[8] R.S. MacKay, J.D. Meiss, Hamiltonian Dynamical Systems, Adam Hilger, Bristol, 1987.
[9] P. Maniadis, T. Bountis, Quasiperiodic and chaotic breathers in a parametrically driven system without linear dispersion, Phys. Rev. E 73 (2006) 046211.
[10] T. Manos, Ch. Skokos, E. Athanassoula, T. Bountis, in: 19th Panhellenic Conference/Summer School Nonlinear Science and Comlexity, Thessaloniki, Greece, 2007 (nlin/0703037).
[11] Ch. Skokos, J. Phys. A 34 (2001) 10029.
[12] Ch. Skokos, T. Bountis, Ch. Antonopoulos, Physica D 231 (2007) 30.
[13] Ch. Skokos, T. Bountis, Ch. Antonopoulos, European Phys. J. (2008) (in press) (nlin/0802.1646).